JOURNAL OF THERMOPHYSICS AND HEAT TRANSFER
Vol. 7, No. 1, Jan.–March 1993

Validation of Chemistry Models Employed in a Particle Simulation Method

Brian L. Haas* and Jeffrey D. McDonald†
Eloret Institute, Palo Alto, California 94303

A simple validation technique is presented and applied to the chemistry models employed in a statistical particle simulation method as implemented on the Intel iPSC/860 multiprocessor computer. While constrained to match known equilibrium behavior, these models are difficult to validate for transient chemical relaxation due to the scarcity of applicable experimental data. However, simulated transient species concentrations and temperatures in reactive reservoirs may be compared directly to those computed from integration of the corresponding differential reaction rate equations. Chemical relaxation of 5-species air in these reservoirs involves 34 simultaneous dissociation, recombination, and atomic-exchange reactions. The reaction rates employed in the analytic solutions are obtained from Arrhenius experimental correlations as functions of temperature for adiabatic gas reservoirs in thermal equilibrium. In the particle simulation, thermal equilibrium conditions are enforced by augmenting rotational and vibrational relaxation at each time step. Favorable agreement with the analytic solutions validates the simulation when applied to relaxation of O_2 toward equilibrium in reservoirs dominated by dissociation and recombination, respectively, and when applied to relaxation of air in the temperature range 5000–30,000 K.

Nomenclature

AB, . . .	=	chemical species
{AB}	=	mutually orbiting pair of atoms
a	=	constant in Arrhenius correlation
b	=	exponent in Arrhenius correlation
D	=	dissociation bond energy of a molecule
E	=	reservoir thermal energy
E_r	=	activation threshold energy of reaction r
f	=	molecular energy distribution function
g	=	molecular relative translational velocity
K	=	equilibrium concentration coefficient
k	=	Boltzmann constant
k_f	=	forward rate coefficient
n	=	number density
P	=	selection probability function
p	=	gas pressure
r	=	reaction index
$S_{a,b}$	=	number of pairs of species a and b in cell
s	=	species index
T	=	temperature
t	=	time
X	=	collision partner species
Z	=	volumetric collision rate
α	=	exponent of intermolecular potential
β	=	leading constant in probability functions
Δt	=	time step increment
$\delta_{a,b}$	=	Kronecker delta
ε	=	individual molecular energies
ζ	=	number of thermal DOF
θ_v	=	characteristic vibrational temperature
λ_0	=	initial gas mean free path
μ	=	reduced mass
ν	=	stoichiometric coefficient
ρ_0	=	initial gas density
σ	=	cross-section constant

Subscripts

a, b	=	pair of species a and b
C, D, R	=	collision, dissociation, recombination
e	=	equilibrium concentration
int	=	internal energy modes
max	=	maximum index
s	=	species s
r	=	reaction r
0	=	initial or freestream value

Superscripts

*	=	equilibrium value
′	=	reaction products
t	=	time step

Introduction

SIMULATION of extremely rarefied flows at high temperatures is afforded by application of statistical particle simulation methods. In the DSMC method of Bird,[1] phenomenological microscopic models are employed to capture appropriate macroscopic flow behavior including thermal and chemical relaxation. Variants of this method have been developed for improved computational performance with vector- and parallel-processing computer architectures.[2–5] In particular, the method of Baganoff and McDonald[6] has recently been implemented on the Intel iPSC/860 parallel-processing computer[7] and is capable of simulating multidimensional reactive gas mixtures employing several million particles. The objective of this article is to outline and apply a simple technique to validate this recent implementation for reactive flow simulation.

Particle simulation methods fundamentally decouple molecular motion from molecular interaction.[1] Given a particular position, velocity, and internal energy status, each particle in the flowfield travels unobstructed along the linear trajectory of its velocity vector over the duration of a single time step. At this time, neighboring particles are identified throughout

Presented as Paper 91-1367 at the AIAA 26th Thermophysics Conference, Honolulu, HI, June 24–27, 1991; received Nov. 19, 1991; revision received April 10, 1992.

*Research Scientist, Aerothermodynamics Branch, Mailing Address: NASA Ames Research Center, M/S 230-2, Moffett Field, CA 94035. Member AIAA.

†Research Scientist; currently with MasPar Computer Corp., 749 N. Mary Ave., Sunnyvale, CA 94086. Member AIAA.

the flowfield and paired-off as potential collision candidates. The flowfield is divided into a network of cells to facilitate identification of neighboring particles and to define the finest resolution for sampling macroscopic flow properties. Employing probabilities as functions of individual collision parameters such as collision cross section and relative translational speed,[6] the subset of all candidate pairs which collide during the time step are identified. In a similar manner, the subset of colliding pairs which react are identified by computing a unique reaction probability for each pair as a function of the translational and internal energies contributing to the given collision. Those pairs of colliding particles selected for reaction then experience the corresponding reaction mechanics involving alteration of thermal energy modes and conversion of reactants into products. Nonreactive colliding particles experience thermal collision mechanics which may include rotational and vibrational relaxation.[8-10]

To validate the reaction models of the particle simulation as well as their implementation on the iPSC/860 computer, adiabatic chemical relaxation of thermally-equilibrated air reservoirs is simulated. The resulting transient species concentrations are then compared to those predicted by numerical integration of the corresponding reaction rate equations. These tests isolate the reactive behavior of the gas and permit validation of the chemistry models under conditions for which only limited experimental data is available. Although the simulation is applicable to flows characterized by general thermochemical nonequilibrium, validation of the method under such conditions is difficult and represents a topic of continuing research.[11]

Chemical Reactions in Air

Highly shocked or expanding flows of atmospheric air (neglecting ionization) relax chemically through dissociation and recombination reactions of the form

$$O_2 + X \rightleftharpoons O + O + X \tag{1}$$

$$N_2 + X \rightleftharpoons N + N + X \tag{2}$$

$$NO + X \rightleftharpoons N + O + X \tag{3}$$

where X represents any species playing a catalytic role in the reaction and through exchange reactions of the form

$$NO + O \rightleftharpoons O_2 + N \tag{4}$$

$$NO + N \rightleftharpoons N_2 + O \tag{5}$$

Note that air is modeled here with the five species O_2, N_2, NO, O, and N, though more complete models would include ions such as NO^+.

Associated with each reaction r is an activation threshold energy E_r representing the minimum amount of energy which must be contained within the contributing thermal energy modes of colliding molecules before the reaction may be initiated. Associated with each diatomic species is a dissociation bond energy D which represents the amount of energy required to break the interatomic bond. This energy is surrendered by the thermal energy modes of the contributing molecules upon reaction. Consequently, the activation threshold energy for an endothermic dissociation reaction is equal to the bond energy of the corresponding molecule. This bond energy also represents the amount of exothermic energy absorbed by the molecular thermal energy modes during formation of the diatomic molecule.

Macroscopic Reaction Rates

In a general gas mixture composed of $s_{\max}$ species, r may be written in the form

$$\sum_{s=1}^{s_{\max}} \nu_{s,r} X_s \underset{k_{b,r}}{\overset{k_{f,r}}{\rightleftharpoons}} \sum_{s=1}^{s_{\max}} \nu'_{s,r} X_s \tag{6}$$

Associated with each reaction is a forward rate coefficient $k_{f,r}$ and equilibrium concentration coefficient $K_r \equiv k_{f,r}/k_{b,r}$. In light of the temperature dependence of K_r, the term "equilibrium concentration coefficient" is used here rather than the misleading term "equilibrium constant" typically mentioned in the literature. The rate of generation or destruction of a particular species a due to r at t is determined by the differential rate equation

$$\left(\frac{dn_a}{dt}\right)_r^t = (\nu'_{a,r} - \nu_{a,r}) k_{f,r} \left[\prod_{s=1}^{s_{\max}} (n_s)^{\nu_{s,r}} - \frac{1}{K_r} \prod_{s=1}^{s_{\max}} (n_s)^{\nu'_{s,r}}\right]_r^t \tag{7}$$

The k_f are unique for each reaction and have been observed experimentally (far from equilibrium) to exhibit the temperature-dependence dictated in the Arrhenius form

$$k_f(T) = a_f T^{b_f} \exp[-(E_r/kT)] \tag{8}$$

where a_f, b_f and E_r are constants. Similar behavior at equilibrium is presumed to follow that in Eq. (8). The temperature variation of K is established both by chemical thermodynamics, through the law of mass action and van't Hoff's equation, and by statistical mechanics.[12] Conveniently, this may be approximated by the Arrhenius form

$$K(T) = a_e T^{b_e} \exp[-(D/kT)] \tag{9}$$

with constants a_e, b_e, and D correlated from experiment. The present work employs k_f tabulated by Park and Menees[13] and K tabulated by Vincenti and Kruger.[12]

Given that there are $r_{\max}$ simultaneous reactions occurring in the mixture, the net change in species a due to all reactions collectively is given per unit volume by the sum

$$\left(\frac{dn_a}{dt}\right)^t = \sum_{r=1}^{r_{\max}} \left(\frac{dn_a}{dt}\right)_r^t \tag{10}$$

Simulation of Reservoir Chemistry

A constant-volume, adiabatic reservoir of gas in chemical nonequilibrium will relax toward equilibrium through reactions as described above. If the gas is artificially maintained at thermal equilibrium then a single gas T may be identified. As a result, the macroscopic k_f and K may be readily computed from their respective Arrhenius forms as functions of T. It is therefore possible to simultaneously integrate the differential rate equations from Eqs. (7) and (10) numerically, leading to transient species concentrations during chemical relaxation of the reservoir. Likewise, the reactive reservoir may be simulated with the particle method and the validity of its solution may be compared directly to that obtained by way of numerical integration of the rate equations.

Analytic Solution of Reaction Rate Equations

At equilibrium the translational and internal energy modes per species contribute to the total E as follows:

$$E = \sum_{s=1}^{s_{\max}} \frac{n_s}{n} \left(\frac{3}{2} kT + \frac{\zeta_{\text{int}_s}}{2} kT\right) \tag{11}$$

The internal DOF ζ_{int} include contributions from rotational and vibrational energy modes[12] given by

$$\zeta_{\text{int}_s} = \begin{cases} 0, & \text{if } s \text{ is monatomic} \\ 2 + 2\dfrac{\theta_{v,s}/T}{\exp(\theta_{v,s}/T) - 1} & \text{if } s \text{ is diatomic} \end{cases} \tag{12}$$

where the vibrational mode is modeled by the simple harmonic oscillator with quantum level increments of energy $k\theta_{v,s}$.

Neither the analytic development here nor the particle simulation method is limited to the simple harmonic oscillator description of the vibrational mode.[11] Such a model is employed only for simplicity in this study of transient chemical behavior under conditions of thermal equilibrium.

During a reaction the creation and destruction of diatomic species is accompanied by the addition or removal of D from the total energy in an adiabatic reservoir. Consequently, the rate of change of E is given by

$$\frac{dE}{dt} = \sum_{s=1}^{s_{max}} \left(\frac{dn_s}{dt} D_s \right) \tag{13}$$

At a given time, T^t is well-defined and uniform among all energy modes of all species for a gas in thermal equilibrium. Consequently, the reaction coefficients of Eqs. (8) and (9) may be computed, leading to determination of the reaction rates from Eqs. (10) and (13). At $t + 1$, the species concentrations and the reservoir energy are approximated from the rate of change of n_a due to all reactions at the previous step t by way of first-order Euler integration

$$n_a^{t+1} = n_a^t + \left(\frac{dn_a}{dt} \right)^t \Delta t \tag{14}$$

$$E^{t+1} = E^t + \sum_{s=1}^{s_{max}} (n_s^{t+1} - n_s^t) D_s \tag{15}$$

The temperature T^{t+1} associated with the next time step is then found by iteration from Eq. (11). In the particle simulation, the length of Δt is governed by the condition that the collision probabilities must never exceed unity. Since reaction rates are significantly slower than collision rates this same Δt is sufficiently small as to lead to stable and accurate solutions of the difference equations in Eqs. (14) and (15).

Particle Simulation of Reservoir Chemistry

Transient thermal-equilibrium conditions are simulated in the particle method by allowing for rapid thermal relaxation relative to chemical relaxation. To achieve this in the simulation, all particles experience two or more additional thermal collisions at the end of each time step. These auxiliary collisions involve exhanges of energy between the translational, rotational, and vibrational energy modes to promote thermal equilibrium[8-10] such that all modes may be described by a single temperature.

Multidimensional flowfield simulations typically employ roughly 20–200 particles per cell. Once the simulation has achieved steady state, reliable macroscopic flow properties such as temperature and density are sampled by averaging them over several time steps for a given cell. However, time-averaging with so few particles is troublesome in combustion flows where trace amounts of catalytic species greatly influence the reaction processes. Though not well-suited to particle simulation methods, such problems may be addressed (with some difficulty) by employing weighting factors for species of low concentration. It is also inappropriate, however, to employ time-averaging when studying the transient behavior inherent to the reservoir simulations here. Therefore, it is necessary to employ a greater number of particles (as many as 80,000) in the single-cell reservoirs of the present study in order to generate meaningful statistics by way of ensemble-averaging. These two schemes for statistical averaging are equivalent in typical steady-state airflows where species of extremely low concentrations do not dominate the chemical kinetics in the gas. Correspondingly, the results of the present study serve to validate the air chemistry models employed in practical implementations of the simulation method.

Chemical reactions are modeled in particle simulation methods by selecting a subset of colliding pairs to react. Pairs of neighboring particles (of species a and b) are selected for collision by computing a unique collision probability P_c for each pair and comparing it to a uniform random number for acceptance or rejection. Derived from the inverse power-law intermolecular potential of exponent α, the form of P_c is given by[6]

$$P_c = \frac{n_a n_b}{1 + \delta_{a,b}} \frac{\sigma_{a,b} \Delta t}{S_{a,b}} g^{1 - 4/\alpha_{a,b}} \tag{16}$$

Here, $S_{a,b}$ is the number of $a + b$ pairs formed in a given cell, and g is the relative translational speed of impact for the given pair. Note that α may vary from the Maxwell molecule limit ($\alpha = 4$) to the hard-sphere limit ($\alpha = \infty$). The cross-section parameter $\sigma_{a,b}$ is related to the resulting collision rate $Z_{a,b}$ per unit volume as follows:

$$Z_{a,b} = \frac{n_a n_b}{1 + \delta_{a,b}} \sqrt{\frac{4}{\pi}} \left(\frac{2kT}{\mu_{a,b}} \right)^{1/2 - (2/\alpha_{a,b})} \sigma_{a,b} \Gamma \left(2 - \frac{2}{\alpha_{a,b}} \right) \tag{17}$$

where $\mu_{a,b} \equiv m_a m_b/(m_a + m_b)$ is the reduced mass of the colliding pair.

The rate of dissociation of species AB due to collisions with partners of species X is dependent upon the dissociation probability P_D and is related to the collision rate as follows:

$$\frac{dn_{AB}}{dt} = -n_{AB} n_X k_f = Z_{AB,X} \int_{E_r}^{\infty} P_D(\varepsilon_C) f_C^*(\varepsilon_C) \, d\varepsilon_C \tag{18}$$

Here, ε_C is the collision energy comprised of relative translational, rotational, and vibrational molecular energies of the pair, and is distributed at equilibrium in the Boltzmann distribution $f_C^*(\varepsilon_C)$ with ζ_C DOF; that is

$$\varepsilon_C = \tfrac{1}{2} \mu_{AB,X} g^2 + \varepsilon_{int_{AB}} + \varepsilon_{int_X} \tag{19}$$

$$\zeta_C = 4 - \frac{4}{\alpha_{AB,X}} + \zeta_{int_{AB}} + \zeta_{int_X} \tag{20}$$

Note the dependence of the relative translational energy upon the intermolecular potential exponent α. A convenient form of P_D which satisfies Eq. (18), when k_f is of the form in Eq. (8), is given by[14]

$$P_D = \beta_D \left(1 - \frac{E_r}{\varepsilon_C} \right)^{(\zeta_C/2) - 1} (\varepsilon_C - E_r)^{\psi} \tag{21}$$

where ψ and β_D are constants given by

$$\psi = b_f - \frac{1}{2} \left(1 - \frac{4}{\alpha} \right) \tag{22}$$

$$\beta_D = \frac{(1 + \delta_{AB,X}) \alpha_f \sqrt{\frac{\pi}{4}} \left(\frac{\mu}{2k} \right)^{1/2 - (2/\alpha)} \Gamma \left(\frac{\zeta_C}{2} \right)}{\sigma \Gamma \left(2 - \frac{2}{\alpha} \right) \Gamma \left(\frac{\zeta_C}{2} + \psi \right) k^{\psi}} \tag{23}$$

Note that $\alpha \equiv \alpha_{AB,X}$, $\sigma \equiv \sigma_{AB,X}$, and $\mu \equiv \mu_{AB,X}$ pertain to the AB + X collision. Note also that ζ_C exhibits very weak temperature-dependence and may therefore be evaluated at some reference temperature T_{ref}, defined by any intermediate translational temperature in the gas. An appropriate selection probability for atomic-exchange reactions is identical in form to that for dissociation in Eq. (21).

The recombination model of the present work is adapted from the model of Bird[15] and employs psuedospecies representing pairs of mutually orbiting atoms. Three-body recombination reactions are then modeled as a succession of in-

dependent binary collision events. On one time step, colliding atoms A and B form a mutually orbiting pair, denoted in braces as {AB}. Recombination may be completed during the next time step through stabilization of {AB} upon collision with partner X as follows:

$$A + B \rightarrow \{AB\} \tag{24}$$

$$\{AB\} + X \rightarrow AB + X \tag{25}$$

Those orbiting pairs {AB} which do not stabilize during the next time step simply split into free atoms. It must be verified that this method captures the appropriate ternary collision behavior associated with recombination while retaining the computational simplicity of binary collision selection and mechanics.

The recombination/stabilization probability P_R is related to the collision rate $Z_{\{AB\},X}$ and the rate of formation of molecules AB as follows:

$$\frac{dn_{AB}}{dt} = n_A n_B n_X \frac{k_f}{K} = Z_{\{AB\},X} \int_0^\infty P_R(\varepsilon_C) f_C^*(\varepsilon_C)\, d\varepsilon_C \tag{26}$$

Here, ε_C is composed of all energy modes contributing to the collision of orbital pair {AB} with partner X, and is distributed at equilibrium with ζ_C DOF

$$\varepsilon_C = \tfrac{1}{2}\mu_{\{AB\},X} g^2 + \varepsilon_{int\{AB\}} + \varepsilon_{int_X} \tag{27}$$

$$\zeta_C = 4 - \frac{4}{\alpha_{\{AB\},X}} + 4 - \frac{4}{\alpha_{A,B}} + \zeta_{int_X} \tag{28}$$

Note that the internal energy of the orbital pair $\varepsilon_{int\{AB\}}$ simply represents the relative translational energy of the monatomic A + B collision. Collision rate $Z_{\{AB\},X}$ is dependent upon $n_{\{AB\}}$ which is itself related to the monatomic collision rate $Z_{A,B}$ as follows:

$$\frac{dn_{\{AB\}}}{dt} = Z_{A,B} \Rightarrow n_{\{AB\}} = Z_{A,B}\Delta t \tag{29}$$

In light of the expressions for $Z_{a,b}$, k_f, and K given above, an appropriate form of recombination probability P_R is as follows:

$$P_R = \beta_R(\varepsilon_C)^{-\phi} \tag{30}$$

where constants ϕ and β_R are given by

$$\phi = 1 - \frac{2}{\alpha_{A,B}} - \frac{2}{\alpha_{\{AB\},X}} + b_c - b_f \tag{31}$$

$$\beta_R = \frac{\pi(1 + \delta_{A,B})\left(\frac{a_f}{a_c}\right)\Delta t}{2^{3 - (2/\alpha_{A,B}) - (2/\alpha_{\{AB\},X})} k^{b_f - b_c}} \times \frac{(\mu_{A,B})^{1/2 - (2/\alpha_{A,B})}(\mu_{\{AB\},X})^{1/2 - (2/\alpha_{\{AB\},X})}}{\sigma_{A,B}\sigma_{\{AB\},X}} \times \frac{\Gamma\left(\frac{\zeta_C}{2}\right)}{\Gamma\left(2 - \frac{2}{\alpha_{\{AB\},X}}\right)\Gamma\left(2 - \frac{2}{\alpha_{A,B}}\right)\Gamma\left(\frac{\zeta_C}{2} - \phi\right)} \tag{32}$$

Note that the selection probabilities are defined in terms of Arrhenius parameters a_f, b_f, a_c, and b_c. While there is considerable uncertainty as to the appropriate experimental values of these parameters, nonetheless, improved estimates of them will readily lead to improved reaction probabilities employed in the particle simulation method. Likewise, the net reaction rate behavior is constrained to match the specified Arrhenius form regardless of the particular values of collision parameters α and σ employed in the simulation.

Reservoir Results and Comparisons

Several reservoirs were simulated to test the chemistry models over a considerable range of temperature. The initial reservoir conditions characterizing each case are listed in Table 1. Results are presented first for dissociation-dominated chemical relaxation of O_2, followed by recombination-dominated relaxation of a nearly monatomic reservoir of oxygen. Isolating these two chemical processes during relaxation toward equilibrium rigorously validates each model independently. Finally, the significance of exchange reactions and the effects of multiple species on the reaction models are best observed in simulated reservoirs of five-species air during chemical relaxation.

In each reservoir case, λ_0 was set equal to the width of one cell. A length scale which relates this simulation parameter to the mean free path in the physical domain is typically determined from experimental observations of the temperature-dependence of gas viscosity.[12,16] However, the length scales employed in the reservoir simulations were adjusted to promote more rapid chemical relaxation relative to the molecular collision rate. Consequently, the collision cross-section parameter $\sigma_{a,b}$ was enhanced such that fewer elastic collisions were required between reactive collisions. This minimized computational cost by reducing the number of time steps required to capture significant chemical behavior. The net reaction rates in both the particle simulation and the analytic solutions were unaffected by this scaling.

Dissociation-Dominated Relaxation of O_2

A reservoir of purely diatomic oxygen at high temperature which relaxes toward equilibrium primarily through dissociation reactions was simulated with the particle method (case 1). The transient species concentrations and reservoir temperature are plotted against time in Figs. 1 and 2. Note that the species concentrations at any given time t are plotted as number density normalized by the initial total number density of the reservoir n_s^1/n^0. Comparison to the numerical solution of the analytic differential equations from Eqs. (14) and (15) indicates favorable agreement. As expected for endothermic reactions, the reservoir temperature drops dramatically in time as dissociation removes thermal energy from the gas.

Near equilibrium, the reservoir is composed primarily of oxygen atoms. In the simulation fewer than 10% of those atoms temporarily reside in mutually orbiting pairs employed in the recombination model.

Recombination of Monatomic Oxygen

A reservoir composed primarily of monatomic oxygen will relax toward equilibrium through chemical relaxation dominated by recombination reactions. Species concentrations and reservoir temperatures are plotted against time in Figs. 3 and 4 for simulation case 2. The initial density and pressure simulated in this case are rather high in order to promote an equilibrium state with a significant diatomic concentration. Such conditions provide a more rigorous challenge for the recombination models than would be encountered for simulations at lower pressures.

Just as with dissociation, close agreement with the analytic solutions verifies the suitability of the simulation for these reactive conditions. Note that the reservoir temperature rises considerably in time as exothermic reaction energy is transferred to the thermal energy modes of the molecules. Rising temperatures eventually increase the dissociation rate to the point of matching the recombination rate, attaining chemical equilibrium in the reservoir. Again, fewer than 10% of the

Table 1 Reservoir simulation conditions

Case	T_0, K	p_0, atm	ρ, kg/m^3	λ_0, m	Concentration	Δt, s
1	20,000	0.063	1.226×10^{-3}	4.0×10^{-5}	100% O_2	1.520×10^{-9}
2	1,000	5.430	$1.226 \times 10^{+0}$	2.0×10^{-7}	1% O_2, 99% O	2.414×10^{-12}
3	30,000	1.000	1.172×10^{-2}	8.0×10^{-6}	21% O_2, 79% N_2	2.321×10^{-10}
4	20,000	1.000	1.757×10^{-2}	4.0×10^{-6}	21% O_2, 79% N_2	1.421×10^{-10}
5	10,000	1.000	3.515×10^{-2}	2.0×10^{-6}	21% O_2, 79% N_2	1.005×10^{-10}

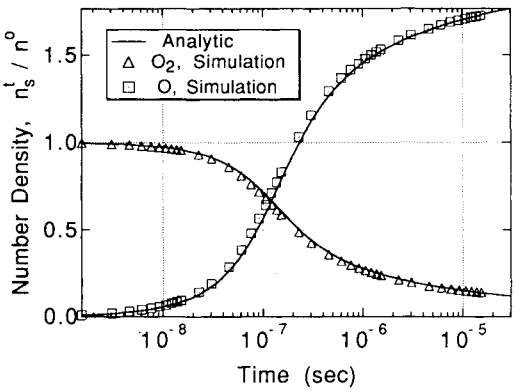

Fig. 1 Species concentrations during chemical relaxation of an O_2 reservoir dominated by dissociation (case 1).

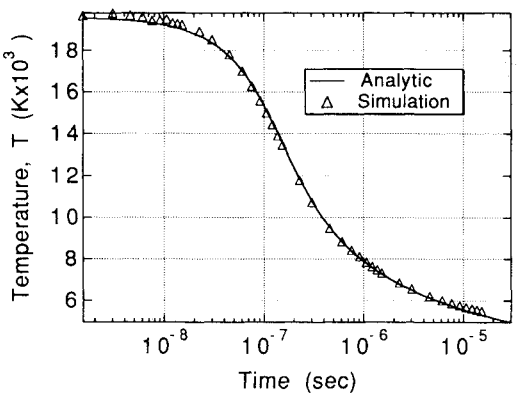

Fig. 2 Temperature during chemical relaxation of an O_2 reservoir dominated by dissociation (case 1).

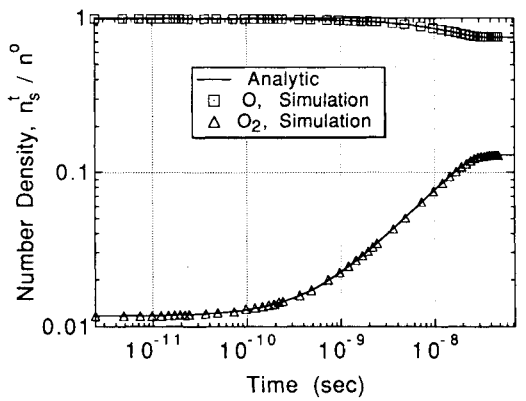

Fig. 3 Species concentrations during chemical relaxation of an O_2 reservoir dominated by recombination (case 2).

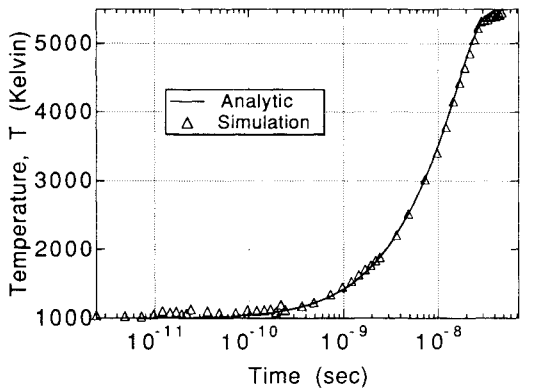

Fig. 4 Temperature during chemical relaxation of an O_2 reservoir dominated by recombination (case 2).

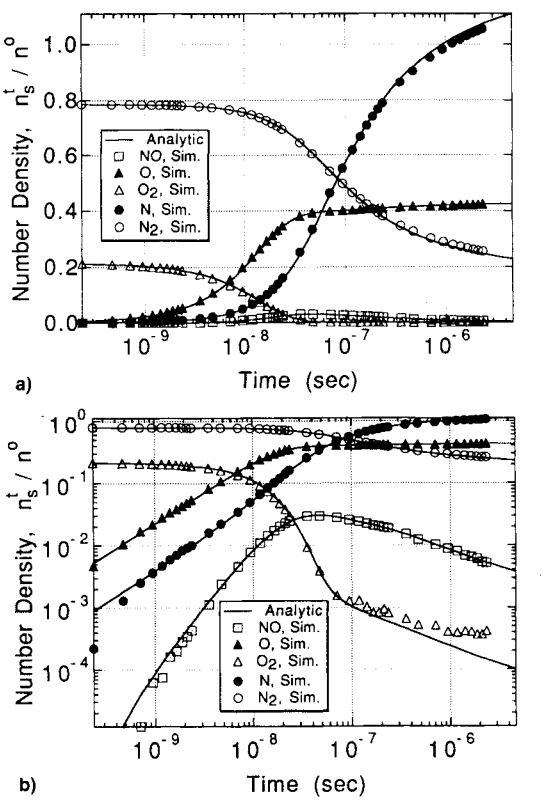

Fig. 5 Species concentrations during chemical relaxation of an air reservoir with initial temperature T_0 = 30,000 K at p_0 = 1 atm (case 3). a) Semilog plot, b) log-log plot.

monatomic species in the reservoir reside in the form of mutually orbiting pairs of atoms at any time. These orbiting pairs, which facilitate efficient modeling of recombination in the simulation, clearly promote the correct macroscopic transient behavior of the relaxing reservoir.

Chemical Relaxation of Air

Reservoirs initialized with number-density concentrations of 21% O_2 and 79% N_2 at high temperatures are qualitatively similar to atmospheric air under highly shocked conditions. Simulation cases 3–5 in Table 1 apply to the chemical relaxation of such reservoirs involving 34 simultaneous dissociation, atomic-exchange, and recombination reactions in general gas mixtures over a considerable range of temperature. Results for each case are presented in Figs. 5–7. Species concentrations are plotted in both log-log and semi-log form to verify transient behavior of dominant species as well as identify statistical limitations associated with lesser species. Interestingly, the transient concentration of a given species is fairly accurately simulated even when there are no more than

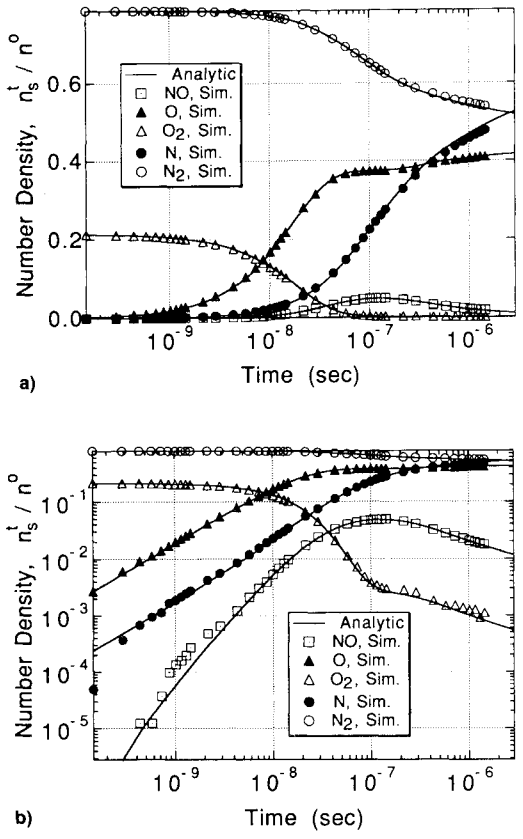

Fig. 6 Species concentrations during chemical relaxation of an air reservoir with initial temperature T_0 = 20,000 K at p_0 = 1 atm (case 4). a) Semilog plot, b) log-log plot.

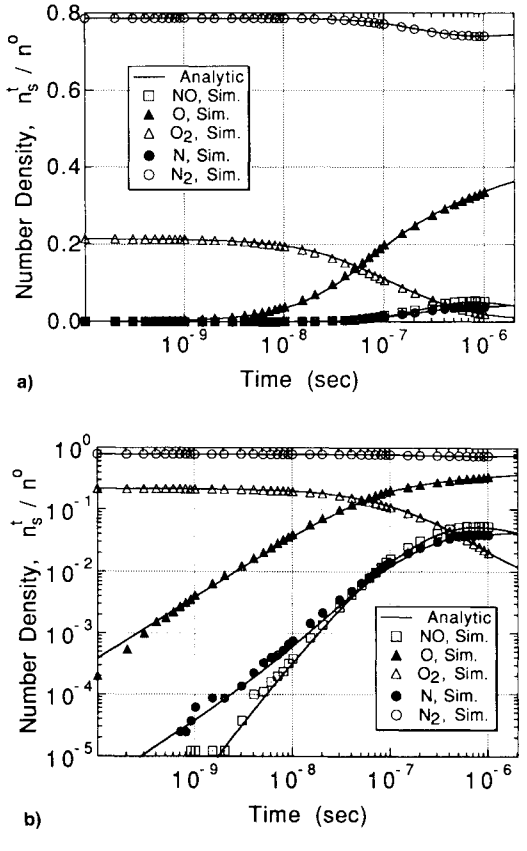

Fig. 7 Species concentrations during chemical relaxation of an air reservoir with initial temperature T_0 = 10,000 K at p_0 = 1 atm (case 5). a) Semilog plot, b) log-log plot.

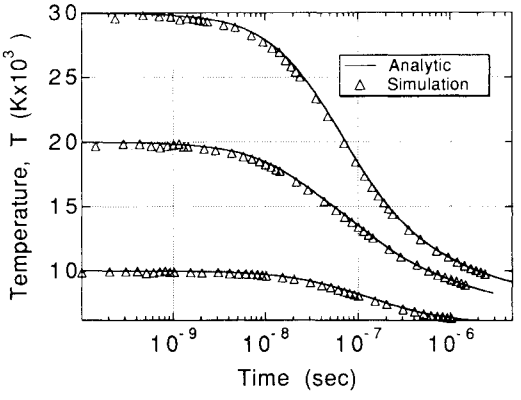

Fig. 8 Temperatures during chemical relaxation of air reservoirs (cases 3, 4, and 5).

10 particles of that species out of a total of 50,000 particles remaining in the reservoir.

Plots of reservoir temperature against time in Fig. 8 verify that the models for reaction mechanics appropriately account for the alteration of molecular thermal energies during reaction. Results for case 3, at high reservoir temperatures, demonstrate considerable chemical activity in the reservoir—particularly that involving nitrogen—in contrast with that occurring at lower temperatures in case 5. Formation of nitric oxide NO in these reservoirs is primarily due to the atomic-exchange reactions of Eqs. (4) and (5) rather than the recombination reactions of Eq. (3).

Concluding Remarks

The particle simulation of Baganoff and McDonald and its implementation on the Intel iPSC/860 multiprocessor computer provides a computationally efficient means of simulating hypersonic rarefied flows. This simulation has been extended for reactive flows by incorporating chemistry selection rules and reaction mechanics models. Unfortunately, attempts to validate particle simulation methods are hampered by the scarcity of experimental data applicable to the flows of interest.

In this article, the ability of the simulation to model reactive flows is partially verified by comparison of simulated species concentrations during adiabatic chemical relaxation of constant-volume reservoirs to those predicted by numerical solution of the corresponding differential reaction rate equations. Results validate the statistical selection rules for dissociation, atomic-exchange, and recombination reactions. Plots of transient reservoir temperatures verify that the models for reaction mechanics appropriately account for the alteration of molecular thermal energies during reaction. These comparisons were facilitated by enforcing thermal equilibrium throughout the chemical relaxation transient. Since the reaction models are defined in terms of experimental Arrhenius coefficients, future improvements in the available experimental data will not alter the agreement observed here. Results of the present study also serve to validate more practical implementations of the particle method which employ steady-state time averaging and fewer particles to simulate air chemistry. More rigorous validation of the simulation would involve thermochemical nonequilibrium which represents a topic of future study. Nonetheless, this validation technique provides a simple and robust test of the fundamental reaction models employed in particle simulation methods.

Acknowledgments

The authors acknowledge and appreciate the support of NASA-Ames Research Center for use of its facilities. This work is sponsored in part (for B.L.H.) by NASA Grant NCC2-582, and (for J.D.M.) by NASA Grant NCC2-674.

References

[1]Bird, G. A., *Molecular Gas Dynamics*, Clarendon Press, Oxford, England, UK, 1976.

[2]McDonald, J. D., "A Computationally Efficient Particle Simulation Method Suited to Vector Computer Architectures," Ph.D. Dissertation, Dept. of Aeronautics and Astronautics, Stanford Univ., Stanford, CA, 1989.

[3]Boyd, I. D., "Vectorization of a Monte Carlo Simulation Scheme for Nonequilibrium Gas Dynamics," *Journal of Computational Physics*, Vol. 96, No. 2, 1991, pp. 411–427.

[4]Dagum, L., "On the Suitability of the Connection Machine for Direct Particle Simulation," Ph.D. Dissertation, Dept. of Aeronautics and Astronautics, Stanford Univ., Stanford, CA, 1990.

[5]Wilmoth, R., "Application of a Parallel DSMC Method to Hypersonic Rarefied Flows," AIAA Paper 90-0772, Reno, NV, Jan. 1991.

[6]Baganoff, D., and McDonald, J. D., "A Collision-Selection Rule for a Particle Simulation Method Suited to Vector Computers," *Physics of Fluids A*, Vol. 2, No. 7, 1990, pp. 1248–1259.

[7]McDonald, J. D., "Particle Simulation in a Multi-Processor Environment," AIAA Paper 91-1366, Honolulu, HI, June 1991.

[8]Haas, B. L., "Fundamentals of Chemistry Modeling Applicable to a Vectorized Particle Simulation," AIAA Paper 90-1749, Seattle, WA, June 1990.

[9]Haas, B. L., "Models of Energy-Exchange Mechanics Applicable to a Particle Simulation of Reactive Flow," *Journal of Thermophysics and Heat Transfer*, Vol. 6, No. 2, 1992, pp. 200–207.

[10]Haas, B. L., "Thermochemistry Models Applicable to a Vectorized Particle Simulation," Ph.D. Dissertation, Dept. of Aeronautics and Astronautics, Stanford Univ., Stanford, CA, 1990.

[11]Haas, B. L., and Boyd, I. D., "Models for Vibrationally-Favored Dissociation Applicable to a Particle Simulation," AIAA Paper 91-0774, Reno, NV, Jan. 1991.

[12]Vincenti, W. G., and Kruger, C. H., *Introduction To Physical Gas Dynamics*, Wiley, New York, 1965.

[13]Park, C., and Menees, G. P., "Odd Nitrogen Production by Meteoroids," *Journal of Geophysical Research*, Vol. 83, No. C8, 1978, pp. 4029–4035.

[14]Bird, G. A., "Simulation of Multi-Dimensional and Chemically Reacting Flows," *Rarefied Gas Dynamics*, edited by R. Campargue, Vol. 1, Commissariat A L'Energie Atomique, Paris, France, 1979, pp. 365–388.

[15]Bird, G. A., "Direct Molecular Simulation of a Dissociating Gas," *Journal of Computational Physics*, Vol. 25, No. 4, 1977, pp. 353–365.

[16]Bird, G. A., "Definition of Mean Free Path for Real Gases," *Physics of Fluids*, Vol. 26, No. 11, 1983, p. 3222, 3223.